[Submitted conference paper summary, January 1997.]

Modeling dynamic receptive field changes produced by intracortical microstimulation

George J. Kalarickal **Jonathan A. Marshall**

Department of Computer Science, CB 3175, Sitterson Hall
University of North Carolina, Chapel Hill, NC 27599-3175, U.S.A.
919-962-1954, kalarick@cs.unc.edu, marshall@cs.unc.edu

Abstract

Intracortical microstimulation (ICMS) of a localized site in the somatosensory cortex of rats and monkeys for 2–6 hours produces a large increase in the cortical representation of the skin region represented by the ICMS-site neurons before ICMS, with very little effect on the ICMS-site neuron's RF location, RF size, and responsiveness (Recanzone et al., 1992). The "EXIN" (afferent excitatory and lateral inhibitory) learning rules (Marshall, 1995) are used to model RF changes during ICMS. The EXIN model produces reorganization of RF topography similar to that observed experimentally. The possible role of inhibitory learning in producing the effects of ICMS is studied by simulating the EXIN model with only lateral inhibitory learning. The model also produces an increase in the cortical representation of the skin region represented by the ICMS-site RF. ICMS is compared to artificial scotoma conditioning (Pettet & Gilbert, 1992) and retinal lesions (Darian-Smith & Gilbert, 1995), and it is suggested that lateral inhibitory learning may be a general principle of cortical plasticity.

1 Introduction

1.1 Receptive field topography changes during intracortical microstimulation

Intracortical microstimulation (ICMS) of a localized site in the somatosensory cortex of rats and monkeys produces reorganization of receptive field (RF) topography over a large region of the cortex (Recanzone et al., 1992). ICMS excites nearly all afferents and excitatory and inhibitory cortical neurons within a few microns of the stimulating electrode. This stimulation produces nearly simultaneous activation of all pre- and postsynaptic elements and modulatory inputs close to the ICMS site. In addition, some of the afferent terminals receive ortho- and antidromic excitation. However, not all anti- and orthodromically excited afferents succeed in driving their target neurons above threshold (Recanzone et al., 1992). ICMS of the cortex for 2–6 hours produces a large (2-fold to over 20-fold) increase in the cortical representation of the skin region represented by the ICMS-site neurons before ICMS (Recanzone et al., 1992).

1.2 EXIN model of dynamic RFs changes during ICMS

We have formulated and tested a neural network model that exhibits similar RF topographical changes. The model, which uses the EXIN (excitatory+inhibitory) learning rules (Marshall, 1995), predicts some experimentally testable RF characteristics. The EXIN model uses modifications in the synaptic efficacy of feedforward excitatory and lateral inhibitory connection pathways to describe the effects of ICMS.

A novel feature of the EXIN model is the role of lateral inhibitory learning rule. We have used the EXIN lateral inhibitory learning to model dynamic RF changes produced by artificial scotoma conditioning and retinal lesions (Darian-Smith & Gilbert, 1995; Marshall & Kalarickal, 1997; Pettet & Gilbert, 1992). Recanzone et al. (1992) realized a need for different learning in excitatory and inhibitory synapses during ICMS to account for all the results. However, they did not propose any specific rule for modifying inhibitory synapses.

2 Methods

We simulated a patch of somatosensory cortical neurons, arranged in a 30×30 grid of spatial positions. The position of each neuron's RF corresponded to the neuron's position in the grid. Adjacent RFs initially had more than 50% spatial overlap.

During ICMS some neurons (excitatory and inhibitory) and afferent terminals are directly activated by the electrical current, and others are activated/receive input indirectly through synaptic activation or via anti- and orthodromic activations of thalamocortical afferents (Recanzone et al., 1992). The neurons receive a combination of direct and indirect excitation and inhibition. Therefore, in the simulations, ICMS was modeled by

1. activating cortical neurons close to the ICMS site;
2. anti- and orthodromically activating all branches of thalamocortical afferents terminating on the directly activated cortical neurons; and
3. directly inhibiting excitatory neurons.

Neurons also receive indirect excitation and inhibition via synaptic activations. The strength of the direct and indirect excitation and inhibition is maximum at the ICMS site and decreases with distance from the ICMS site according to a Gaussian function. The Gaussian distribution of the direct and indirect excitatory and inhibitory strengths is based on the observation that the strength of electrical stimulation decreases with distance from the stimulation site (Recanzone et al., 1992).

The spread of direct excitation and inhibition is small; indirect excitation and inhibition spread over a large distance. In the model as well as in the experimental data, the indirect presynaptic excitations spread over large distances, but most are initially ineffective in driving cortical neurons.

2.1 Simulation procedure

To simulate ICMS, direct excitation and inhibition are held constant. The indirect excitation and inhibition via synapses change during ICMS because the strength of synapses change according to the EXIN learning rules.

2.2 The EXIN learning rules

2.2.1 The EXIN lateral inhibitory learning rule

The EXIN lateral inhibitory learning rule (Marshall, 1995) is an anti-Hebbian outstar learning rule. The weight Z_{ij}^{-} of the lateral inhibitory pathway from neuron i to neuron j is governed by the following equation:

$$\frac{d}{dt} Z_{ij}^{-} \;=\; \delta g(x_i) \left(-Z_{ij}^{-} + q(x_j) \right), \tag{1}$$

where $\delta > 0$ is a small learning rate constant, x_i and x_j are the activation levels of neurons i and j, respectively, and g and q are half-rectified increasing functions. Thus, *whenever a neuron is active, its output inhibitory connections to other active neurons tend to become slightly stronger (i.e., more inhibitory), while its output inhibitory connections to inactive neurons tend to become slightly weaker.*

In an outstar learning rule (Grossberg, 1972), *pre*synaptic activity "enables" the learning at a synapse; when the learning is enabled, the weight tends to become proportional to the postsynaptic activity. In an instar learning rule, *post*synaptic activity enables the learning; when the learning is enabled, the weight tends to become proportional to the presynaptic activity. Thus, in an instar rule, the subscripts for x_i and x_j in the equation above would be interchanged.

2.2.2 The EXIN feedforward excitatory learning rule

The afferent excitatory pathway weight changes are governed by the EXIN excitatory learning rule, which is an instar Hebbian rule. The rule can be expressed (Grossberg, 1982; Marshall, 1995) as

$$\frac{d}{dt} Z_{ij}^{+} = \epsilon f(x_j) \left(-Z_{ij}^{+} + h(x_i) \right), \tag{2}$$

where i is a modeled thalamic neuron and j is a modeled cortical neuron, x_i and x_j are the activation levels of neurons i and j, respectively, Z_{ij}^{+} is the feedforward excitatory weight from neuron i to neuron j,

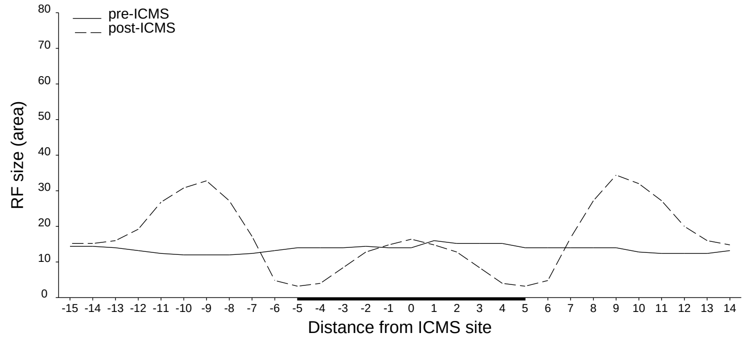

Figure 1: **Changes in RF size.** The figure shows the RF area of neurons in a cross-section of cortex passing through the ICMS site before and after ICMS. The thick line on the abscissa represents the neurons active during the initial phase of ICMS.

$\epsilon > 0$ is a small learning rate constant, and f and h are half-rectified increasing functions. Thus, *whenever a neuron is active, its input excitatory connections from active neurons become slightly stronger, while its input excitatory connections from inactive neurons become slightly weaker.*

2.3 The activation equation

The activation level x_j of each modeled cortical neuron is governed by a shunting equation (Grossberg, 1972) based on the Hodgkin-Huxley model:

$$\frac{d}{dt}x_q = -Ax_q + \beta(B - x_q)E_q - \gamma(C + x_q)I_q, \tag{3}$$

where A, B, C, β, and γ are positive constants, and E_j and I_j represent respectively the neuron's total excitatory and inhibitory input signals. Because Equation 3 is a shunting equation, neuron activation levels remain within a bounded range, between $-C$ and B.

3 Results

3.1 Synaptic reorganization during ICMS in the EXIN model

During ICMS three distinct types of synaptic modification occur in the EXIN model.

1. The EXIN inhibitory learning rule decreases the weights of the lateral inhibitory pathways from the active neurons to the surrounding inactive neurons. This decrease in inhibitory weights to the initially inactive neurons allows these neurons to respond to the excitation they receive via anti- and orthodromically activated afferents. In addition, the decreased inhibition causes an expansion in the RF size of these neurons and thereby an increase in RF overlap with the ICMS-site RF. However, the lateral inhibitory weights from the inactive neurons to active neurons do not change. Thus, as the RFs of the previously inactive neurons expand toward the ICMS-site RF, the neighboring active neurons receive more inhibition, and their RFs contract (Figure 1).

2. According to the EXIN feedforward excitatory learning rule, the active cortical neurons during ICMS strengthen excitatory synapses from the strongly active afferents at the ICMS site or the branches of the afferents at the ICMS site and weaken excitatory synapses from weakly active and inactive afferents. Thus, during ICMS the RFs of the active neurons shift to overlap with the ICMS-site RF. Neurons closest to the ICMS site eventually have RFs almost identical to the ICMS-site RF (Figures 1 & 2). This dramatic change in RF has been termed "RF substitution" (Recanzone et al. 1992).

3. In response to the relatively weak activation of some neurons during ICMS, the learning rule in the simulation causes the lateral inhibitory weights between the active neurons to weaken. This keeps the RF size and responsiveness of the ICMS-site neurons roughly constant (Figures 1 & 3).

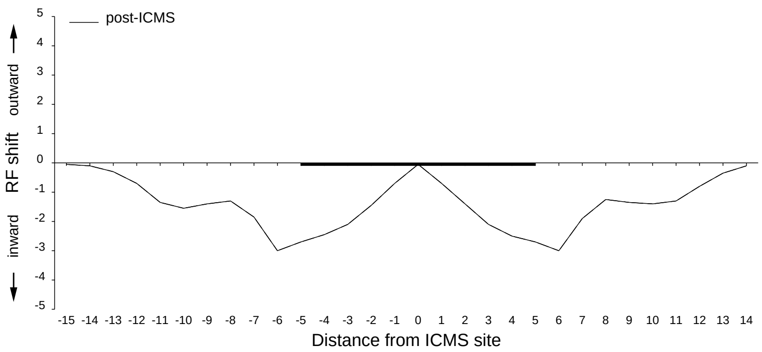

Figure 2: **RF shift after ICMS.** The figure shows the RF shift of neurons in a cross-section of cortex passing through the ICMS site after ICMS. The thick line on the abscissa represents the neurons active during the initial phase of ICMS.

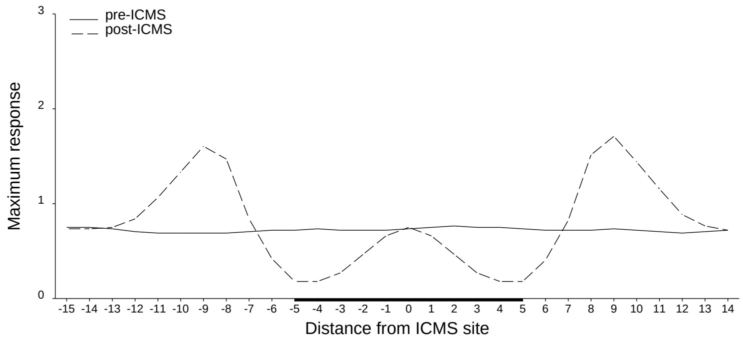

Figure 3: **Changes in neuronal responsiveness after ICMS.** The figure shows the maximum responsiveness of neurons in a cross-section of cortex passing through the ICMS site before and after ICMS. The thick line on the abscissa represents the neurons active during the initial phase of ICMS.

3.2 Comparison of the EXIN model with neurophysiological data

During ICMS, the computational simulation of the EXIN model produced the following effects, corresponding closely to the experimental neurophysiological results reported by Recanzone et al. (1992):

- increase in the cortical representation of the ICMS-site RF (Figure 4);
- almost no change in RF size and responsiveness of ICMS-site neuron (Figures 1 & 3);
- substitution of the ICMS-site RF for the former RF of surrounding neurons (Figures 1 & 2);
- RF expansion in some neurons and contraction in others (Figure 1); and
- RF shift toward the ICMS-site RF (Figure 2).

With no learning in excitatory synapses and learning in inhibitory synapses, the model predicts an increase in the number of cortical neurons with RFs overlapping with the ICMS-site RF. An experimental idea is to abolish learning in excitatory synapses without affecting inhibitory learning by injecting an NMDA antagonist into the cortex during ICMS. NMDA antagonists have been shown to abolish changes in excitatory synaptic efficacy without completely eliminating postsynaptic responses to electrical and visual stimulation (Bear et al., 1992; Dudek & Bear, 1992). To draw firm conclusions, controls would be required to estimate changes in excitatory and inhibitory synapses.

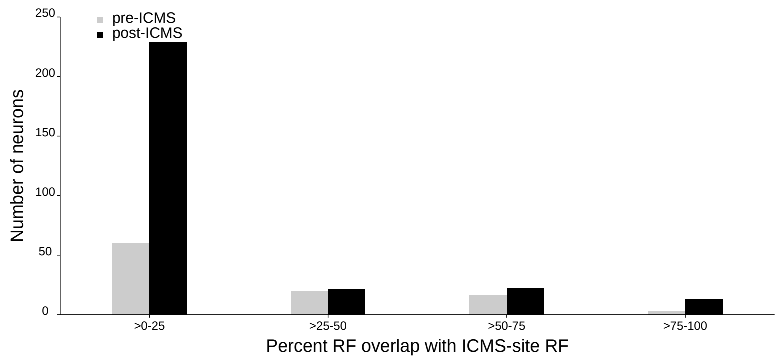

Figure 4: **Changes in RF overlap with the ICMS-site RF.** The figure shows the number of simulated cortical neurons with RF overlapping with the ICMS-site RF before and after ICMS.

4 Discussion

The EXIN model reproduces the main effects of ICMS on cortical RF location, size, and responsiveness. The combination of the EXIN afferent excitatory and lateral inhibitory learning produces an increase in the cortical representation of the skin region corresponding to the ICMS site, without much effect on ICMS-site RF size and responsiveness.

The EXIN model predicts an increase in the cortical representation of the skin region corresponding to the ICMS site, even with no afferent excitatory learning. A neurophysiological experiment abolishing learning in excitatory synapses without shutting down learning in inhibitory synapses would test the predictions of the EXIN lateral inhibitory learning rule. Other experiments to verify the predictions of the EXIN learning rule have been proposed by Marshall and Kalarickal (1997).

This work, in conjunction with the EXIN model of artificial scotoma conditioning and retinal lesions (Marshall & Kalarickal, 1997), suggests the hypothesis that outstar lateral inhibitory plasticity is an important and general principle in cortical organization.

References

[1] Bear, M.F., Press, W.A., & Connors, B.W. (1992) Long-term potentiation in slices of kitten visual cortex and the effects of NMDA receptor blockade. *Journal of Neurophysiology*, **67(4)**, 841–851.

[2] Darian-Smith, C. & Gilbert, C.D. (1995) Topographic reorganization in the striate cortex of the adult cat and monkey is cortically mediated. *The Journal of Neuroscience*, **15(3)**, 1631–1647.

[3] Dudek, S.M. & Bear, M.F. (1992) Homosynaptic long-term depression in area CA1 of hippocampus and effects of N-methyl-D-aspartate receptor blockade. *Proceedings of the National Academy of Sciences USA*, **89**, 4363–4367.

[4] Grossberg, S. (1972) Neural expectation: Cerebellar and retinal analogs of cells fired by learnable or unlearned pattern classes. *Kybernetik*, **10**, 49–57.

[5] Grossberg, S. (1982) *Studies of Mind and Brain: Neural Principles of Learning, Perception, Development, Cognition, and Motor Control*, Reidel Press: Boston, MA.

[6] Marshall, J.A. (1995) Adaptive perceptual pattern recognition by self-organizing neural networks: Context, uncertainty, multiplicity, and scale. *Neural Networks*, **8**, 335–362.

[7] Marshall, J.A. & Kalarickal, G.J. (1997) Modeling dynamic receptive field changes in primary visual cortex using inhibitory learning. To appear in *Computational Neuroscience '96*, J. Bower (ed.), Plenum, New York.

[8] Pettet, M.W. & Gilbert, C.D. (1992) Dynamic changes in receptive-field size in cat primary visual cortex. *Proceedings of the National Academy of Sciences USA*, **89**, 7, 8366–8370.

[9] Recanzone, G.H., Merzenich, M.M., & Dinse, H.R. (1992) Expansion of the cortical representation of a specific skin field in primary somatosensory cortex by intracortical microstimulation. *Cerebral Cortex*, **2**, 181–196.